

In Situ Raman Investigation on the Structural Transformation of Oxovanadium Hydrogenphosphate Hemihydrate in the Presence of Ammonia

Yue Zhang,[†] Manfred Meisel,[†] Andreas Martin,^{*,‡} Bernhard Lücke,[‡] Klaus Witke,[§] and Klaus-Werner Brzezinka[§]

Humboldt Universität zu Berlin, Institut für Anorganische und Allgemeine Chemie, Hessische Strasse 1-2, D-10115 Berlin, Germany; Institut für Angewandte Chemie Berlin-Adlershof e.V., Rudower Chaussee 5, D-12484 Berlin, Germany; and Bundesanstalt für Materialforschung und -prüfung, Rudower Chaussee 6, D-12489 Berlin, Germany

Received November 13, 1996. Revised Manuscript Received February 25, 1997[®]

Raman spectra of the transformation of oxovanadium hydrogenphosphate hemihydrate, $\text{VOHPO}_4 \cdot \frac{1}{2}\text{H}_2\text{O}$, were measured in an in situ Raman cell under an ammonia/oxygen/helium flow in the presence of water vapor at temperatures up to 723 K. During the thermal treatment a decomposition of the parent structure proceeds as indicated by a distinct broadening and disappearing of the parent Raman bands. After holding the sample for 1 h under these conditions and during subsequent cooling, the structural transformation into $(\text{NH}_4)_2[(\text{VO})_3(\text{P}_2\text{O}_7)_2]$ is observed. After allowing this to stand at room temperature under flowing helium for some hours, V_2O_5 and mainly NH_4VO_3 particles (up to 100 μm) are formed as new phases. Both are spatially separated from the $(\text{NH}_4)_2[(\text{VO})_3(\text{P}_2\text{O}_7)_2]$ surface as detected by means of the micro-Raman technique. It seems very likely that NH_4VO_3 is generated from in situ existing V(V) particles and chemisorbed ammonia.

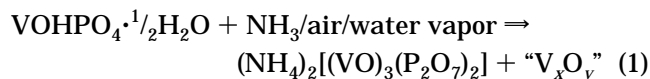
Introduction

$\text{VOHPO}_4 \cdot \frac{1}{2}\text{H}_2\text{O}$ has long been used as a precursor compound to generate $(\text{VO})_2\text{P}_2\text{O}_7$ catalysts employed in the selective oxidation of *n*-butane to maleic anhydride (e.g., ref 1). Recently, the effect of $\text{VOHPO}_4 \cdot \frac{1}{2}\text{H}_2\text{O}$ as a potential ammoxidation catalyst precursor was studied.^{2–4} It was found first by X-ray diffraction (XRD) that during the ammoxidation of methylaromatics a structural transformation from $\text{VOHPO}_4 \cdot \frac{1}{2}\text{H}_2\text{O}$ into an ammonium-containing oxovanadium pyrophosphate (identified as $(\text{NH}_4)_2[(\text{VO})_3(\text{P}_2\text{O}_7)_2]$) proceeded.² After the transformation, the $(\text{NH}_4)_2[(\text{VO})_3(\text{P}_2\text{O}_7)_2]$ showed a constant activity and selectivity in the ammoxidation of various substituted toluenes to the corresponding nitriles. Otherwise, the observed catalyst activity and selectivity strongly depend on the kind of the methylaromatic reactant fed, i.e., the size and the electronic as well as the steric properties of different substituents (e.g., $-\text{OCH}_3$ and $-\text{Cl}$) influence the reaction immensely.^{5,6}

In our previous paper, an investigation of this phase transformation has been reported using XRD and

spectroscopic methods such as Raman and FTIR spectroscopy.⁷ It was found, that the structural transformation of $\text{VOHPO}_4 \cdot \frac{1}{2}\text{H}_2\text{O}$ into $(\text{NH}_4)_2[(\text{VO})_3(\text{P}_2\text{O}_7)_2]$, taking place under ammoxidation conditions, is a complicated solid-state reaction, passing through an intermediate phase characterized by a layerlike structure with intercalation of ammonia (cf. ref 8). The formation of this intermediate phase and the presence of a sufficient concentration of water vapor in the gas phase prevent the dehydration of the hemihydrate into $(\text{VO})_2\text{P}_2\text{O}_7$. Moreover, the presence of a sufficient concentration of water vapor seems to be necessary for the transformation: Otherwise, only a very poor crystallinity of the formed $(\text{NH}_4)_2[(\text{VO})_3(\text{P}_2\text{O}_7)_2]$ was observed.⁷ Furthermore, it was proven that this transformation can proceed not only during the ammoxidation reaction but also during heating of the hemihydrate in ammonia/air/water vapor atmosphere, i.e., in the absence of the aromatic reactant.⁷

Apart from $(\text{NH}_4)_2[(\text{VO})_3(\text{P}_2\text{O}_7)_2]$, a vanadium-rich phase should be formed according to the vanadium/phosphorus ratio of the precursor phase and the equilibrated catalyst as shown in eq 1.



It was proposed that the additional phase must be a mixed-valent $\text{V}^{\text{IV}}/\text{V}^{\text{V}}$ -containing vanadium oxide, because the determination of the vanadium valence state of the equilibrated catalyst revealed a value of approximately 4.1.⁷ Recently, an in situ EPR study

[†] Humboldt Universität zu Berlin.

[‡] Institut für Angewandte Chemie Berlin-Adlershof e.V.

[§] Bundesanstalt für Materialforschung und -prüfung.

[®] Abstract published in *Advance ACS Abstracts*, April 1, 1997.

(1) *Vanadyl pyrophosphate catalysts*, Centi, G., Ed.; *Catal. Today* **1993**, 16.

(2) Martin, A.; Lücke, B.; Seeboth, H.; Ladwig, G.; Fischer, E. *React. Kinet. Catal. Lett.* **1989**, 38, 33.

(3) Martin, A.; Lücke, B.; Wolf, G.-U.; Meisel, M. *Catal. Lett.* **1995**, 33, 349.

(4) Lücke, B.; Martin, A. In *Catalysis of Organic Reactions*; Scaros, M. G., Prunier, M. L., Eds.; Chemical Industries Ser.; Marcel Dekker: New York, 1995; Vol. 62, p 479.

(5) Martin, A.; Lücke, B. In *Catalysis of Organic Reactions*; Malz, Jr., R. E., Ed.; Chemical Industries Ser.; Marcel Dekker: New York, 1996; Vol. 68, p 451.

(6) Martin, A.; Lücke, B. *Catal. Today* **1996**, 32, 279.

(7) Zhang, Y.; Martin, A.; Wolf, G.-U.; Rabe, S.; Worzala, H.; Lücke, B.; Meisel, M.; Witke, K. *Chem. Mater.* **1996**, 8, 1135.

(8) Gulianti, V. V.; Benziger, J. B.; Sundarasan, S. *Chem. Mater.* **1994**, 6, 353.

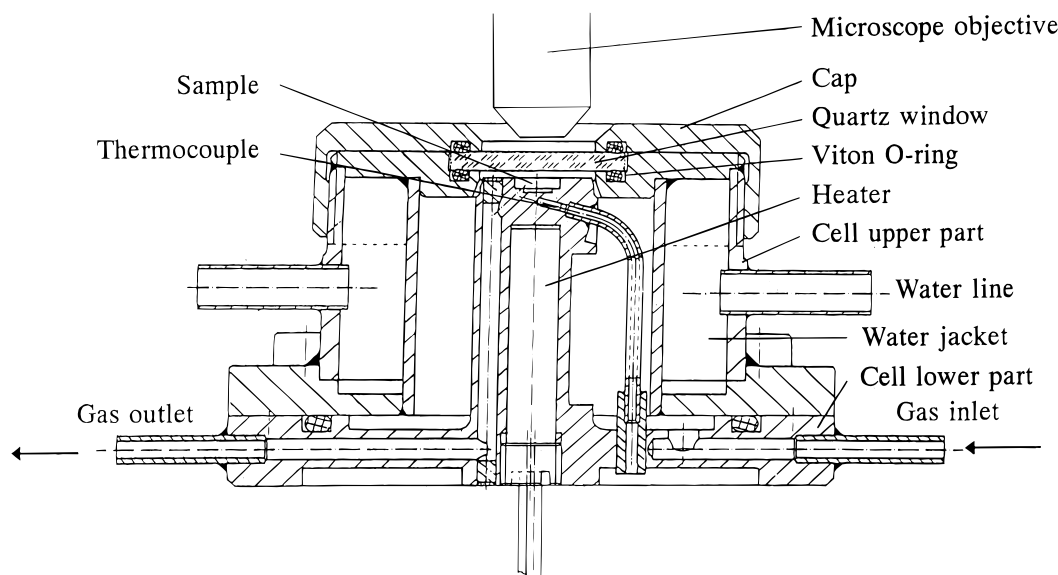


Figure 1. In situ Raman cell in cross-section.

(ammonoxidation of toluene) of the structural transformation of $\text{VOHPO}_4 \cdot \frac{1}{2}\text{H}_2\text{O}$ into $(\text{NH}_4)_2[(\text{VO})_3(\text{P}_2\text{O}_7)_2]$ as well as the investigation of the ammonoxidation reaction, using other ammonium-containing oxovanadium phosphates and vanadium oxides indicated that such a mixed-valent vanadium oxide could be V_4O_9 .⁹

The present work deals with an in situ study of the above-mentioned structural transformation process by means of Raman spectroscopy which has been proven to be an effective method in the catalyst structural analysis and in the understanding of the mechanism of catalytic reactions [e.g., refs 10 and 11]. By using Raman spectroscopy, many works emerged in the literature in recent years, especially in the investigation of vanadium oxides as well as vanadium phosphate catalysts applied in various oxidation reactions [e.g., refs 12–15]. Furthermore, this study points to the determination of the vanadium-rich phase formed during the transformation process and tries a structural conception of the transformation reaction as well.

Experimental Section

The synthesis procedure of $\text{VOHPO}_4 \cdot \frac{1}{2}\text{H}_2\text{O}$ using an aqueous medium^{16,17} and the one of pure $(\text{NH}_4)_2[(\text{VO})_3(\text{P}_2\text{O}_7)_2]$ have been reported previously.⁷

The Raman spectra were obtained with a DILOR-XY-spectrometer (Fa. DILOR, Bensheim) coupled with a nitrogen

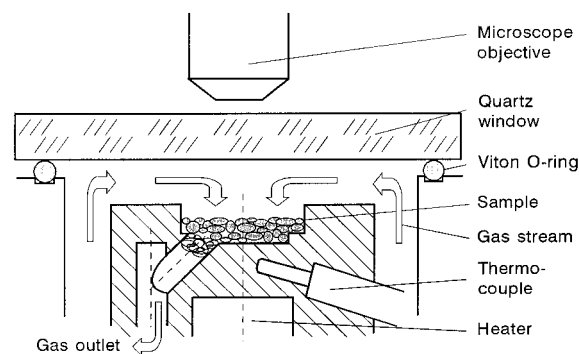


Figure 2. Enlarged diagram of the sample holder section.

cooled ccd camera as detector. The samples were excited using the 514.5 nm line from an ILA 120 argon ion laser (Fa. Carl Zeiss, Jena). 180° backscatter geometry of the micro-Raman technique (Olympus 10× objective, diameter of the laser focus $\approx 10 \mu\text{m}$) was applied to record spectra with high lateral resolution of the powder samples. The microscope is equipped with an Olympus camera, allowing us to take a photo instead of a spectrum of a chosen surface area of the sample positioned in the reticule.

To study the transformation process under reaction conditions, an in situ Raman cell was developed which can be heated to 823 K (Figure 1). The preheated gas stream flows through the catalysts specimens, i.e., the sample could be placed on a stainless steel net or the gas outlet of the sample holder is closed by quartz wool. In both cases, the solid is passed by the gas stream from the top downward. Figure 2 depicts an enlarged diagram of the sample holder section of the in situ Raman cell and illustrates the direction of the gas flow. The in situ Raman cell is connected with a gas manifold system so that the sample could be treated with the premixed and preheated reaction gas feed while the Raman spectra were recorded. The cell is mounted on the microscope desk, allowing the positioning of each point of the sample surface into the reticule of the microscope.

Sample local heating due to high incident laser power can easily induce unwanted changes in the solid morphology or lead to a falsification of the desired reaction temperature.¹⁸ To avoid the thermal influence of laser rays on the precursor transformation studies, a small power level (2.5 mW) was used to record the spectra. The indicated laser power was measured before the entrance optics. With the used objective, the laser beam focal point diameter was approximately 10 mm. The

(9) Brückner, A.; Martin, A.; Steinfeld, N.; Wolf, G.-U.; Lücke, B. *J. Chem. Soc., Faraday Trans.* **1996**, 92, 4251.

(10) Stencel, J. M. *Raman Spectroscopy for Catalysis*; Van Nostrand Reinhold Catalysis Series; VNR: New York, 1990.

(11) Niemantsverdriet, J. W. *Spectroscopy in Catalysis*; VCH: Weinheim, 1993; p 208.

(12) Benabdelouahab, F. B.; Olier, O.; Guilhaume, N.; Lefebvre, F.; Volta, J.-C. *J. Catal.* **1992**, 134, 151.

(13) Jehng, J.-M.; Deo, G.; Weckhuysen, B. M.; Wachs, I. E. *J. Mol. Catal. A* **1996**, 110, 41.

(14) Hutchings, G. J.; Desmartin-Chomel, A.; Olier, R.; Volta, J.-C. *Nature* **1994**, 368, 151.

(15) Birkeland, K. E.; Kung, H. H.; Bare, S. R.; Coulston, G. W.; Harlow, R.; Lee, P. L. In *Symposium on Heterogeneous Hydrocarbon Oxidation Presented before the Division of Petroleum Chemistry, Inc.*; 211th ACS National Meeting; American Chemical Society: New Orleans, LA, March 1996; p 197.

(16) Schlesinger, K.; Ladwig, G.; Meisel, M.; Kubias, B.; Weinberger, R.; Seeboth, H. DP-WP 256.659, 1984.

(17) Berndt, H.; Büker, K.; Martin, A.; Brückner, A.; Lücke, B. *J. Chem. Soc., Faraday Trans.* **1995**, 91, 725.

(18) Kip, B. J.; Meier, R. J. *Appl. Spectrosc.* **1990**, 44, 707.

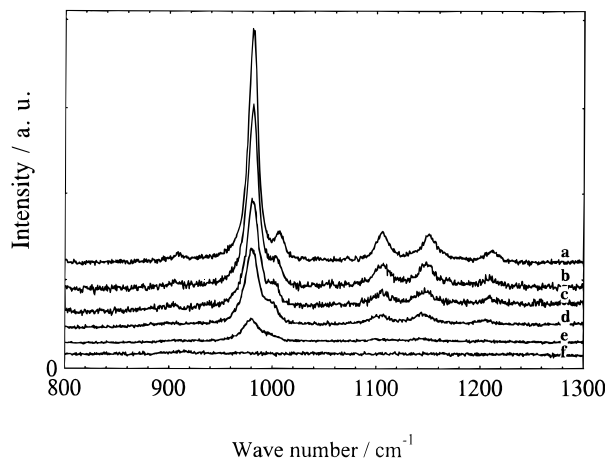


Figure 3. In situ Raman spectra of $\text{VOHPO}_4 \cdot \frac{1}{2}\text{H}_2\text{O}$ transformation obtained during thermal treatment (heating rate $\beta = 25$ K/min; (a) 298 K, (b) 423 K, (c) 523 K, (d) 623 K, (e) 673 K, and (f) 723 K; held for 30 min at each temperature) under an ammonia/oxygen/helium ($\text{NH}_3\text{:O}_2\text{:He} = 1.2\text{:}2\text{:}7$) flow in the presence of water vapor (ca. 20 vol. %).

power level corresponded to an irradiation density of about 0.9 kW/cm^2 , taking into account scattering losses between the entrance optics and the sample. Thus, the local temperature increase on the precursor/catalyst material was negligible. Data acquisition time was up to 200 s according to the intensity of the Raman scattering. Before recording the spectra, the homogeneity of the samples was monitored by measuring the Raman signals at various places. Sample amounts of 10–20 mg were used for each measurement. In the present work, the structural transformation of $\text{VOHPO}_4 \cdot \frac{1}{2}\text{H}_2\text{O}$ was carried out under a flowing gas mixture of ammonia/oxygen/helium ($\text{NH}_3\text{:O}_2\text{:He} = 1.2\text{:}2\text{:}7$) in the presence of water vapor (ca. 20 vol. %) at temperatures up to 723 K (heating rate $\beta = 25$ K/min; held for 30 min each at several temperatures for collecting the Raman spectra). Raman spectra of reference samples were recorded at room temperature in the usual way.

Results and Discussion

The Raman spectra obtained during the thermal treatment of $\text{VOHPO}_4 \cdot \frac{1}{2}\text{H}_2\text{O}$ under the ammonia/oxygen/water vapor/helium flow are presented in Figure 3. The bands at 982 and 1007 cm^{-1} are characteristic for the $\text{VOHPO}_4 \cdot \frac{1}{2}\text{H}_2\text{O}$ precursor (spectrum a, room temperature). Heating of the sample to 723 K (heating rate $\beta = \text{ca. } 25 \text{ K/min}$) results first in a broadening of the bands (e.g., spectrum c, 523 K) and in the end in a disappearance of the Raman signals (spectrum f, 723 K) due to a decomposition of the parent structure. The Raman spectrum becomes structureless. After holding for ca. 1 h under these conditions slight bands at 920 and ca. 980 cm^{-1} appear (spectrum a, 723 K) as depicted in Figure 4. The further spectra were taken during a subsequent cooling program with stops at various temperatures (673, 623, 523, and 423 K and room temperature) for 0.5–1 h each under the mentioned flow (except of water vapor at lower temperatures). The bands at ca. 860 , 914 , and 977 cm^{-1} grow during the cooling period, indicating a further crystallization of $(\text{NH}_4)_2[(\text{VO})_3(\text{P}_2\text{O}_7)_2]$. It is obvious that the applied temperature program and the flowing gas atmosphere lead first to a material that substantially is in an amorphous state after reaching the final temperature. Only a minor amount of crystallized $(\text{NH}_4)_2[(\text{VO})_3(\text{P}_2\text{O}_7)_2]$ could be observed at this time. After the

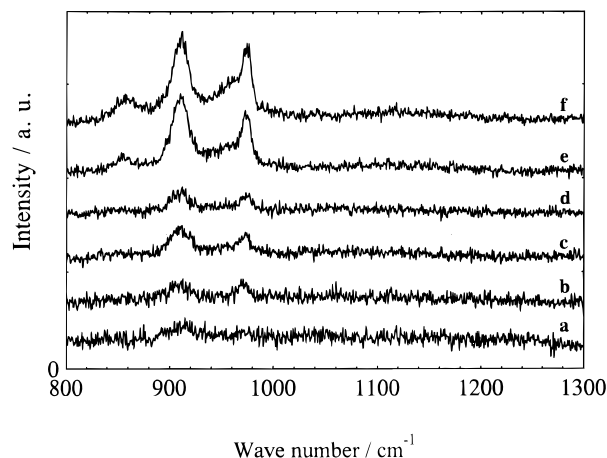


Figure 4. In situ Raman spectra of the $\text{VOHPO}_4 \cdot \frac{1}{2}\text{H}_2\text{O}$ transformation product recorded at various temperatures (a) 723 K, (b) 673 K, (c) 623 K, (d) 523 K, (e) 423 K, and (f) 298 K; held for 30 min at each temperature) during cooling (after 1 h stop at 723 K) under the gas flow mentioned in Figure 3.

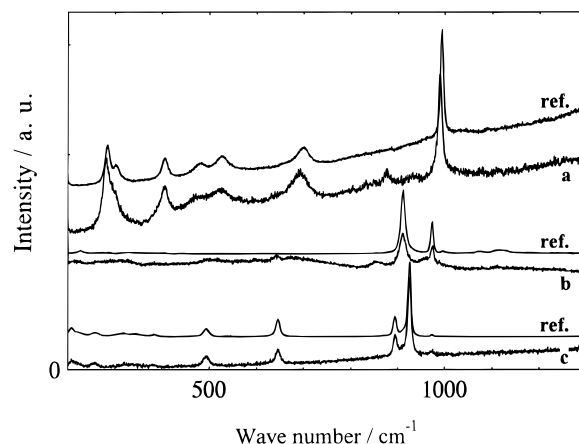


Figure 5. Raman spectra of the three detectable transformation products at room temperature ((a) V_2O_5 , (b) $(\text{NH}_4)_2[(\text{VO})_3(\text{P}_2\text{O}_7)_2]$, and (c) NH_4VO_3 (the lower ones, respectively) and the authentic reference substances (the upper ones, respectively; denoted as ref.).

complete transformation, the generated $(\text{NH}_4)_2[(\text{VO})_3(\text{P}_2\text{O}_7)_2]$ is thermostable; however, its Raman bands are detectable even at 723 K under the above-mentioned gas atmosphere. Furthermore, the heating of the pure, as-synthesized $(\text{NH}_4)_2[(\text{VO})_3(\text{P}_2\text{O}_7)_2]$ under the same conditions shows no significant structural changes up to 803 K.

After cooling to room temperature as described above, only the characteristic bands of $(\text{NH}_4)_2[(\text{VO})_3(\text{P}_2\text{O}_7)_2]$ could be identified (Figure 4, spectrum f). Nevertheless, some new Raman bands were observed besides those related to $(\text{NH}_4)_2[(\text{VO})_3(\text{P}_2\text{O}_7)_2]$ after flushing the sample with He at room temperature overnight. The high lateral resolution allows the recording of spectra of different phases visible under the microscope as particles of a different habit with diameters of about $5\text{--}100 \mu\text{m}$. The spectra of three pure phases obtained in this way are depicted in Figure 5 (a, V_2O_5 ; b, $(\text{NH}_4)_2[(\text{VO})_3(\text{P}_2\text{O}_7)_2]$; c, NH_4VO_3) and are compared with that of the authentic corresponding reference compounds (denoted as ref.). Figure 6 shows a photo of two formed NH_4VO_3 crystals observed under the microscope of the spectrometer; the Raman spectrum of one of them is depicted in Figure 5 as well (spectrum c, lower curve).

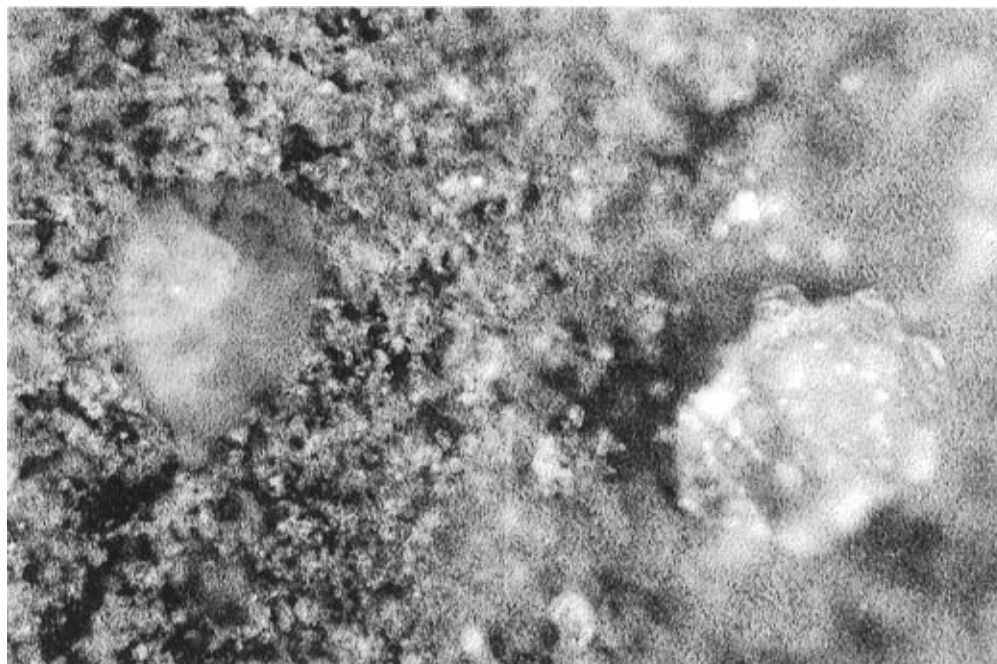


Figure 6. Crystals of the formed NH_4VO_3 under the microscope of the Raman spectrometer (diameter of the crystals ca. $100\ \mu\text{m}$).

Evidently, some of V(V) compounds were formed parallel to the generation of the $(\text{NH}_4)_2[(\text{VO})_3(\text{P}_2\text{O}_7)_2]$ during the transformation of the hemihydrate. The main part of such V(V) compounds found at room temperature was NH_4VO_3 . The amount of V_2O_5 observed certainly depends on the ammonia partial pressure of the feed stream and the cooling conditions. Thus, low ammonia partial pressure as well as cooling under inert gas should inhibit the metavanadate formation due to a lack of chemisorbed ammonia (ammonium ions).

Indeed, the formation of such ammonium metavanadate species on the described route is very likely because recent in situ XRD experiments, proceeding under comparable reaction conditions revealed the formation of crystalline NH_4VO_3 as well.¹⁹ Otherwise, a flushing of the sample at the transformation temperature of 713 K with an inert gas flow for 30 min before cooling, i.e., chemisorbed ammonia was removed/desorbed, showed no such generation of NH_4VO_3 . Thus, in this case the formation of amorphous V_2O_5 proportions after cooling seems to be rather likely, because no XRD pattern of NH_4VO_3 as well as V_2O_5 could be observed.¹⁹

However, under the selected conditions of this investigation, eq 2 demonstrates the possible path of the $\text{VOHPO}_4 \cdot \frac{1}{2}\text{H}_2\text{O}$ precursor transformation into $(\text{NH}_4)_2[(\text{VO})_3(\text{P}_2\text{O}_7)_2]$ and the NH_4VO_3 formation from the in situ generated V_2O_5 or V(V)-containing particles and chemisorbed ammonia during the cooling step and at room temperature, respectively.

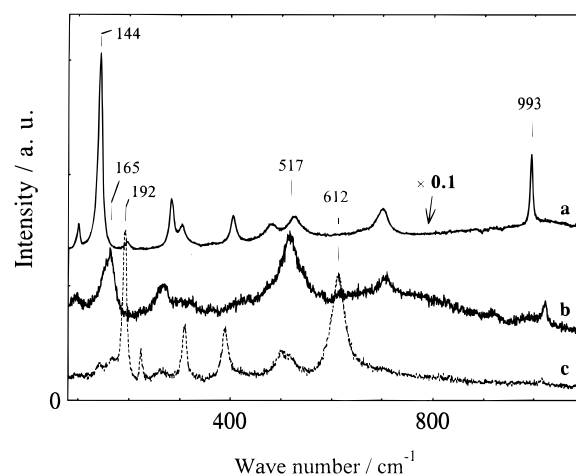
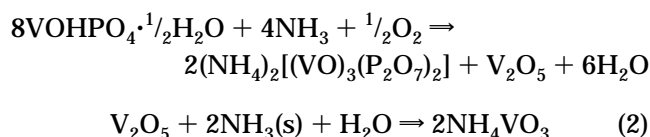


Figure 7. Raman spectra of vanadium oxides ((a) V_2O_5 (note that the ordinate is multiplied by 0.1), (b) V_4O_9 , and (c) VO_2) recorded under identical measuring conditions (laser power 1 mW, integration time: 400 s).

Otherwise, lower-valent vanadium oxides that are not easy to detect by Raman spectroscopy must be also present under the ammonia-containing gas atmosphere as revealed by potentiometric V-valence determination of the final catalyst.⁷ For example, it is very difficult to record intense Raman spectra of V(IV)-containing oxides. This could be one of the causes that only V(V) oxides could be sufficiently observed by means of Raman spectroscopy.

Figure 7 depicts Raman spectra of different vanadium oxides (V_2O_5 , V_4O_9 , and VO_2), illustrating that V(IV)-containing oxides are scarcely able to detect by Raman spectroscopy. This fact is strengthened by the simultaneous presence of V_2O_5 and/or other V(V) compounds as in our case. The structure of VO_2 is built up of VO_6 octahedra, forming a network of the rutile type,²⁰ and

(19) Wilde, L.; Steinike, U.; Martin, A.; Wolf, G.-U.; Lücke, B. *J. Solid State Chem.*, submitted.

(20) Hanuza, J.; Hermanowicz, K.; Oganowski, W.; Jezowska-Trzebiatowska, B. *Bull. Pol. Acad. Sci. Chem.* **1983**, 31, 139.

like that of rutile (TiO_2) the Raman spectrum of VO_2 depends on the orientation of the crystal to the direction of the electric vector of the exciting laser beam. Especially, relative intensities of the lines at 191, 223, 260, and 337 cm^{-1} may be changed by the orientation; spectrum c shows one of some different possibilities.

In our previous work,⁷ we found that ca. 10% of the vanadium of the whole transformation product is in the valence state +5, i.e., ca. 50% of the remaining vanadium (beside the V(IV) proportion that is incorporated in the crystalline $(\text{NH}_4)_2[(\text{VO})_3(\text{P}_2\text{O}_7)_2]$ phase) must be in the valence state +4. This fact was also proven by the mentioned in situ EPR investigations, showing an additional spin-spin exchange of the transformed material in comparison to the pure, as-synthesized compound.⁹ This additional effect must be attributed to V(IV) sites, because V(V) sites are invisible to EPR spectroscopy. However, the final composition of the remaining vanadium oxide phase and the corresponding valence state should depend on the conditions of the transformation, more or less. Furthermore, it is confirmed that in the absence of oxygen the thermal treatment of $\text{VOHPO}_4 \cdot 1/2\text{H}_2\text{O}$ under an atmosphere of ammonia/helium results in the deterioration of its structure and a rapid drop of the V valence state toward V(III) in a short time.

$(\text{NH}_4)_2[(\text{VO})_3(\text{P}_2\text{O}_7)_2]$ is known to be isostructural to the α -modification of $\text{K}_2[(\text{VO})_3(\text{P}_2\text{O}_7)_2]$,⁷ synthesized first by Leclaire et al.²¹ The host lattice can be described in terms of mixed chains $[\text{V}_2\text{P}_8\text{O}_{30}]_x$ linked through $[\text{V}_2\text{O}_{10}]$ units formed from one VO_5 pyramid and one VO_6 octahedron, sharing one corner.²¹ The $[\text{V}_2\text{P}_8\text{O}_{30}]_x$ chains are formed of ReO_3 -type chains connected to pyrophosphate groups. It is known that the structure of $\text{VOHPO}_4 \cdot 1/2\text{H}_2\text{O}$ is built up from couples of VO_6 octahedra, sharing one face linked by PO_4 tetrahedra (e.g., refs 1, 22, and 23). Although different from the structure of $\text{M}_2[(\text{VO})_3(\text{P}_2\text{O}_7)_2]$ ($\text{M} = \text{NH}_4$ or K), $\text{VOHPO}_4 \cdot 1/2\text{H}_2\text{O}$ has similar ReO_3 -type chains but double one sharing the edge of their octahedra.²¹ It seems that a synergistic structural change of two near-neighboring VO_6 couples proceeds during the transformation beside a weakening of the parent layer structure. This process is connected with the intercalation of ammonia that runs under the influence of water vapor, leading to a hydrolytic break of V—O—P links and additional ammonia adsorption after all. During a first step a V(IV) of one octahedron could be oxidized into V(V) which should migrate out of the structure, whereas the other VO_6 octahedron of the ReO_3 -type chain still remains. A second face-shared VO_6 octahedra couple could be transformed into a $[\text{V}_2\text{O}_{10}]$ unit. This process could be imagined in the sense of a study of Benabdelouahab et al.,²⁴ giving a structural idea of the transformation of $\text{VOHPO}_4 \cdot 1/2\text{H}_2\text{O}$ into $\delta\text{-VOPO}_4$ by rocking of PO_4 tetrahedra and inevitable diverging of the VO_6 octahedra. Such structural changes could also happen during $\text{VOHPO}_4 \cdot 1/2\text{H}_2\text{O}$ transformation under the chosen ammonia-containing atmosphere as well as under ammoxidation conditions,

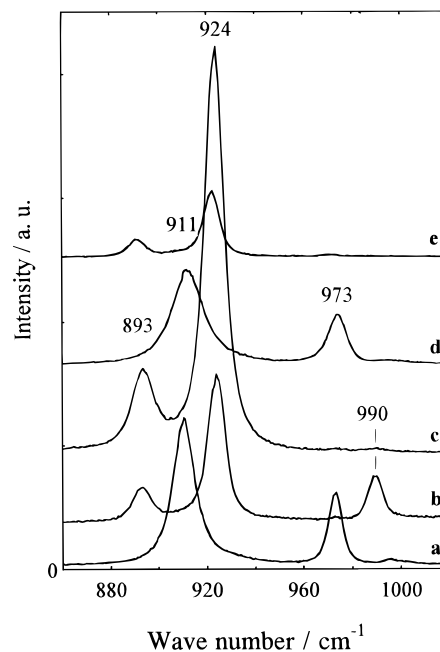


Figure 8. In situ Raman spectra of different surface locations of a 0.5/1 molar mechanical mixture of V_2O_5 and $(\text{NH}_4)_2[(\text{VO})_3(\text{P}_2\text{O}_7)_2]$ under the used gas flow (see Figure 3) and at various temperatures ((a) 298 K, "gray-colored" surface $(\text{NH}_4)_2[(\text{VO})_3(\text{P}_2\text{O}_7)_2]$; (b) 303 K, "orange-colored" particle (V_2O_5 , NH_4VO_3); (c) 423 K, the same particle (only NH_4VO_3); (d) 523 K, only areas of spectrum (a) observable; (e) 298 K, NH_4VO_3 particles are observed again).

probably leading first to the generation of an amorphous phase. Subsequently, a recrystallization takes place, forming $(\text{NH}_4)_2[(\text{VO})_3(\text{P}_2\text{O}_7)_2]$ and the mixed-valent vanadium oxide.

Figure 8 demonstrates the spectra of an in situ Raman experiment with a V_2O_5 -treated $(\text{NH}_4)_2[(\text{VO})_3(\text{P}_2\text{O}_7)_2]$ sample (mechanical mix of V_2O_5 and $(\text{NH}_4)_2[(\text{VO})_3(\text{P}_2\text{O}_7)_2]$ in a molar ratio of 0.5/1) under the same conditions using the above-mentioned ammonia-containing gas flow. At room temperature, the sample shows surface locations, consisting of $(\text{NH}_4)_2[(\text{VO})_3(\text{P}_2\text{O}_7)_2]$ (spectrum a, 910, 972 cm^{-1}) and areas (at slightly higher temperature of 303 K) that reveal the bands of V_2O_5 and surprisingly NH_4VO_3 side by side (spectrum b, 989 cm^{-1} (V_2O_5), 893, 924 cm^{-1} (NH_4VO_3)). This means that a V_2O_5 – NH_3 equilibrium exists even at these low temperatures, leading to the generation of NH_4VO_3 under these conditions. Therefore, it could be expected that NH_4VO_3 is also existent at higher temperatures under an ammonia-containing atmosphere (i.e., above 423 K that was recently given as NH_4VO_3 into V_2O_5 transformation temperature²⁵). Indeed, this assumption is confirmed as shown in the following spectra. At 423 K, the Raman spectrum of V_2O_5 is completely changed to that of NH_4VO_3 (spectrum c, 893, 924 cm^{-1}) which is detectable up to approximately 523 K. Above 523 K only the spectrum of $(\text{NH}_4)_2[(\text{VO})_3(\text{P}_2\text{O}_7)_2]$ could be observed (spectrum d, 911, 973 cm^{-1}), i.e., the previously existing V(V) particles were not to be found anywhere. Probably, these particles will be progressively reduced by ammonia with increasing temperature into V(IV)-containing mixed oxides that are

(21) Leclaire, A.; Chahboun, H.; Groult, D.; Raveau, B. *J. Solid State Chem.* **1988**, 77, 170.

(22) Johnson, J. W.; Johnston, D. C.; Jacobson, A. J.; Brody, J. F. *J. Am. Chem. Soc.* **1984**, 106, 8123.

(23) Bordes, E. *Catal. Today* **1987**, 1, 499.

(24) Benabdelouahab, F.; Volta, J.-C.; Olier, R. *J. Catal.* **1994**, 148, 334.

(25) Lampe-Önnerud, C.; Thomas, J. O. *J. Mater. Chem.* **1995**, 5, 1075.

scarcely able to detect by Raman spectroscopy. However, after cooling the sample to 298 K, the NH_4VO_3 bands appeared again (spectrum e, 893, 924 cm^{-1}). This experiment reveals no indications for V(IV) compounds as well, probably by the same reasons as mentioned above.

Recently, the catalytic properties of different ammonium-containing VPO catalysts (pure $(\text{NH}_4)_2[(\text{VO})_3(\text{P}_2\text{O}_7)_2]$, the equilibrated material of the $\text{VOHPO}_4 \cdot \frac{1}{2}\text{H}_2\text{O}$ transformation and mixtures of pure $(\text{NH}_4)_2[(\text{VO})_3(\text{P}_2\text{O}_7)_2]$ with NH_4VO_3 , produced by impregnating as well as mixing of the solids) were investigated in the ammoxidation of toluene.^{26,27} The pure compound had a very poor activity, whereas the other vanadium oxide-containing samples revealed a significant higher one. The benzonitrile selectivity reached on the pure compound was comparable to that measured on the $\text{VOHPO}_4 \cdot \frac{1}{2}\text{H}_2\text{O}$ transformation product (ca. 95–98%). In contrast, the nitrile selectivity observed on the NH_4VO_3 -containing catalysts decreased to ca. 80% under comparable reaction conditions.²⁶ This is also confirmed by a temporal-analysis-of-products (TAP) followed investigation of the catalytic properties (ammoxidation of toluene) of a prereduced as well as preoxidized $(\text{VO})_2\text{P}_2\text{O}_7$ surface.²⁸ The study clearly showed an increasing catalytic activity but decreasing nitrile selectivity with increasing V(V) content of the surface, whereas a rising V(III) amount inhibits the reaction. An optimum in activity connected with a maximum in nitrile selectivity is reached at an average vanadium valence state, being a little bit above +4. This is also confirmed by potentiometric measurements of used catalysts of similar type, showing an vanadium valence state of approximately +4.1.⁷ However, it seems, that the V(V) species,

primarily generated during the hemihydrate precursor transformation are responsible for the drastic enhancement of the toluene conversion rate in comparison to the pure solid.²⁷

Conclusion

The structural transformation of $\text{VOHPO}_4 \cdot \frac{1}{2}\text{H}_2\text{O}$ into $(\text{NH}_4)_2[(\text{VO})_3(\text{P}_2\text{O}_7)_2]$ was investigated using in situ Raman spectroscopy. The presence of an amorphous state was observed during the transformation. The crystallization of $(\text{NH}_4)_2[(\text{VO})_3(\text{P}_2\text{O}_7)_2]$ from this intermediate phase proceeds slowly. Besides $(\text{NH}_4)_2[(\text{VO})_3(\text{P}_2\text{O}_7)_2]$, some of V(V) compounds such as NH_4VO_3 and V_2O_5 are formed which are observable only at lower temperatures and room temperature, respectively. It seems very likely, that NH_4VO_3 is formed from V(V) particles generated during the transformation and chemisorbed ammonia. The applied micro-Raman technique enables the observation of different surface areas/particles and revealed first time the spatial separation of the $\text{VOHPO}_4 \cdot \frac{1}{2}\text{H}_2\text{O}$ transformation product $(\text{NH}_4)_2[(\text{VO})_3(\text{P}_2\text{O}_7)_2]$ and vanadium oxides (e.g., V_2O_5) as well as NH_4VO_3 at least. A synergistic structural transformation is suggested, in which one V(IV) of a two near-neighborings VO_6 couple unit could be oxidized to V(V) whereas one other VO_6 octahedron still remains in the chain, the other couple could be transformed into the $[\text{V}_2\text{O}_{10}]$ unit of the $(\text{NH}_4)_2[(\text{VO})_3(\text{P}_2\text{O}_7)_2]$ structure.

Acknowledgment. This work was supported by the Federal Ministry of Education, Science, Research, and Technology of the FRG and the Berlin Senate Department for Science, Research, and Culture (Project 03C3005).

CM9605882

(26) Martin, A.; Brückner, A.; Zhang, Y.; *Chem. Ing. Tech.* **1997**, *69*, 97.

(27) Martin, A.; Brückner, A.; Zhang, Y.; Lücke, B. *Stud. Surf. Sci. Catal.*, in press.

(28) Martin, A.; Zhang, Y.; Meisel, M. *React. Kinet. Catal. Lett.*, in press.